AAS 13-860

HALO ORBIT TARGETING GUIDANCE VIA HIGHER ORDER SLIDING TECHNIQUES

Jules Simo* **and Roberto Furfaro** † **and Daniel R. Wibben** ‡

In this paper, the Multiple Sliding Surface Guidance (MSSG) algorithm has been implemented and simulated to verify the ability to target the insertion point of a suitable halo orbit in the vicinity of the Sun-Earth libration points. Based on Higher-Order Sliding Control (HOSC) theory, the proposed MSSG algorithm computes an acceleration command that target a specified state by considering only knowledge of the current and desired position and velocity. Results show that the guidance scheme is able to successfully target a suitable state for proper orbital insertion. Furthermore, it will be shown how the algorithm can be used to target the L_1 point in the Sun-Earth system. A detailed study has also been performed to investigate the guidance performances as function of the guidance parameters. The global stability of the proposed guidance scheme is proven using Lyapunov-based approach.

INTRODUCTION

The design of space missions to remain in the vicinity of an equilibrium point in a three-body system has been a favorite topic over the last decades. The model of the restricted three-body problem has been used extensively in the study of problems of celestial mechanics.[1,2] The initial applications considered a halo orbit near the translunar libration point for a single communications satellite to link the Earth with the far side of the Moon.[3] The Halo orbit is a special case of Lissajous orbit where the in-plane and out-of-plane frequencies are equal.[4,5,6,7,8,9] Using the Earth-Moon System as the primaries in the circular restricted three-body problem, a hybrid concept for displaced lunar orbits has been developed.[10,11,12] A natural extension of the hybrid concept is then to investigate the possible transition to a binary asteroid system, as an application of the restricted problem.[12] Thus, a feedback linearization control scheme was implemented to perform stabilization and trajectory tracking for the nonlinear system.[10,11,12] The first complete orbit aroud the Sun-Earth L_1 point was accomplished by the ISEE-3 (International Sun-Earth Explorer-3) spacecraft in 1979. This laid the groundwork for many later missions, since the Sun-Earth L_1 would be an ideal location to continuously monitor the interplanetary environment upstream from the Earth.

The control issue highlights the multidisciplinary nature of the halo orbit guidance problem. The MSSG algorithm has its theoretical foundation on the well-known sliding control theory,[13] as well on the more recently developed HOSC approach.[14,15,16,17,18,19] Sliding mode Control has been recently employed to develop innovative and more robust algorithms for endo-atmospheric flight system guidance.[18] In particular, sliding mode control methods have emerged as attractive techniques that can be applied to develop robust missile autopilots[18,19] and guidance algorithms.[20,21]

*Academic Visitor, Department of Mechanical and Aerospace Engineering, University of Strathclyde, Glasgow, G1 1XJ, United Kingdom.

†Assistant Professor, Department of Systems and Industrial Engineering, University of Arizona, 1127 E. James E. Roger Way, Tucson, Arizona, 85721, USA.

‡Graduate Student, Department of Systems and Industrial Engineering, University of Arizona, 1127 E. James E. Roger Way, Tucson, Arizona, 85721, USA.

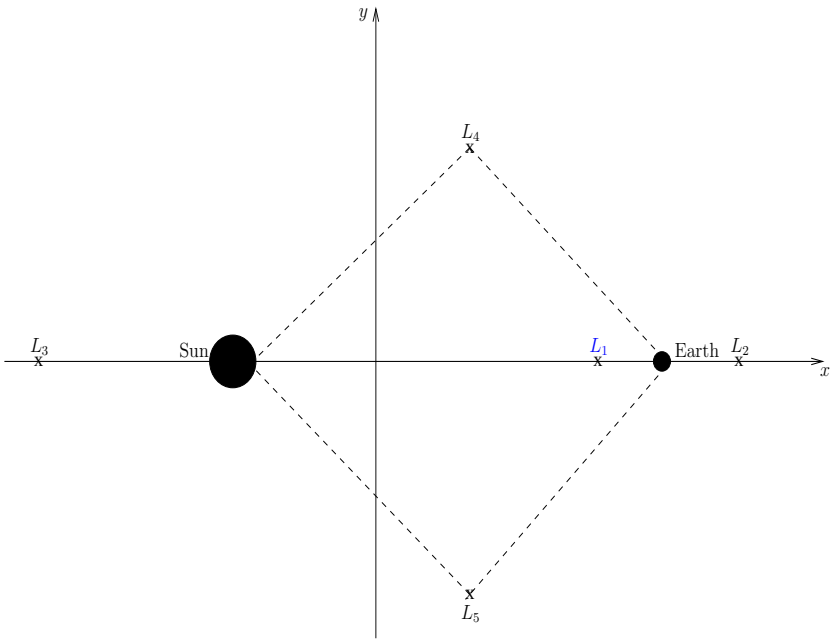

Figure 1. Schematic location of the five Lagrange points in the Sun-Earth System.

However, such non-linear guidance design methods have rarely been used to design guidance algorithms for planetary precision landing. More recently, sliding control theory has been investigated as a mean to develop two classes of robust guidance algorithms for both precision lunar and asteroid landing.[22,23,24,25] Further, the MSSG is designed on the principles of two-sliding mode control, employs multiple sliding surfaces to generate on-line targeting trajectories that are guaranteed to be globally stable under bounded pertubations.[14,15,16,17] Two sliding surface vectors are then concatenated in such a way that an acceleration command that drives the second surface to zero automatically drives the dynamical system on the first surface in a finite time. The on-line trajectory generation and the determination of the guidance command require only knowledge of the current and desired position and velocity.

This paper will use the MSSG optimal guidance scheme to successfully target a suitable state for proper orbital insertion. The next stage involved targeting the L_1 point in the Sun-Earth system for various mission profiles. Moreover, the global stability of the proposed guidance algorithm is proven using a Lyapunov-based approach.

CIRCULAR RESTRICTED THREE-BODY PROBLEM

The circular restricted three-body problem (CRTBP) describes the dynamics of a massless body attracted by two point masses revolving around each other in a circular orbit. In the CRTBP, the motion of a particle (spacecraft) of negligible mass is considered moving under the gravitational influence of two massive bodies, defined as the primaries. It is assumed that the two primaries rotate in circular orbits about their common center of mass. The center of mass is located at the barycenter on the line joining the primaries. The system of interest in this paper is the Sun-Earth system such that m_1 represents the Sun and m_2 represents the Earth, and the motion of a spacecraft of much smaller mass is considered. The unit mass is taken to be the total mass of the system

$(m_1 + m_2)$ and the unit of length is chosen to be the constant separation between m_1 and m_2. The time unit is defined such that m_2 orbits around m_1 in time 2π. Under these considerations the masses of the primaries in the normalized system of units are $m_1 = 1 - \mu$ and $m_2 = \mu$, with $\mu = m_2/(m_1 + m_2)$.

The libration points are the equilibrium solutions of the restricted three-body problem. The three collinear libration points L_1, L_2 and L_3 have been found to exist on the x-axis. The triangular libration points L_4 and L_5 form an equilateral triangle with the two primaries (Figure 1). As already noted, libration points are stationary equilibrium points. It is then possible to find bounded motion in the region of the libration points. The most general motion of this type to be produced in the vicinity of the libration points is a quasi-periodic trajectory.

EQUATIONS OF MOTIONS

Let (x, y, z) be the position of the infinitesimal mass in the rotating frames.The nondimensional equations that govern the motion of the infinitesimal mass in the CRTBP are given by

$$\ddot{x} - 2\dot{y} = x - \frac{1-\mu}{r_1^3}(x+\mu) - \frac{\mu}{r_2^3}(x-1+\mu), \tag{1}$$

$$\ddot{y} + 2\dot{x} = \left(1 - \frac{1-\mu}{r_1^3} + \frac{\mu}{r_2^3}\right) y, \tag{2}$$

$$\ddot{z} = -\left(\frac{1-\mu}{r_1^3} + \frac{\mu}{r_2^3}\right) z, \tag{3}$$

where r_1 and r_2 are equal to the distance from the third body to the primary and secondary, respectively

$$r_1 = \sqrt{(x+\mu)^2 + y^2 + z^2},$$

$$r_2 = \sqrt{(x-1+\mu)^2 + y^2 + z^2}.$$

GUIDANCE MODEL

The fundamental equations of motion of a spacecraft moving in the gravitational field of a planetary body can be described using Newton's law. The equations of motion can be written as

$$\dot{\boldsymbol{r}} = \boldsymbol{v}, \tag{4}$$

$$\dot{\boldsymbol{v}} = 2\boldsymbol{w} \times \boldsymbol{v} + \boldsymbol{w} \times \boldsymbol{w} \times \boldsymbol{r} + \frac{\partial U^T}{\partial \boldsymbol{r}} + \boldsymbol{a}_c + \boldsymbol{a}_p. \tag{5}$$

Here, $\boldsymbol{r} = [x, y, z]^T$ is the position vector in the rotating frame, $\boldsymbol{v} = [v_x, v_y, v_z]^T$ is the velocity vector, $\boldsymbol{a}_c = [a_{cx}, a_{cy}, a_{cz}]^T$ is the acceleration command, and $\boldsymbol{a}_p = [a_{px}, a_{py}, a_{pz}]^T$ is the perturbing acceleration that accounts for unmodeled/unknown forces (e.g., gravity field inaccuracies, solar radiation pressure, and n^{th}-body pertubations).

The equations of motion can be explicitly written in their scalar form as

$$\dot{x} = v_x, \tag{6}$$
$$\dot{y} = v_y, \tag{7}$$
$$\dot{z} = v_z, \tag{8}$$
$$\dot{v}_x = 2wv_y + w^2x + \frac{\partial U}{\partial x} + a_{cx} + a_{px}, \tag{9}$$
$$\dot{v}_y = -2wv_x + w^2y + \frac{\partial U}{\partial y} + a_{cy} + a_{py}, \tag{10}$$
$$\dot{v}_z = \frac{\partial U}{\partial z} + a_{cz} + a_{pz}. \tag{11}$$

The mathematical model described in Eqs. (4-11) is employed to derive the guidance equations.

GUIDANCE ALGORITHM DEVELOPMENT

Sliding Control Theory

The sliding control methodology can be defined as an elementary approach to robust control.[13] Intuitively, it is based on the observation that it is much easier to control non-linear and uncertain first-order systems (i.e., systems described by first-order differential equations) than n^{th}-order systems (i.e., systems described by n^{th}-order differential equations). Generally, if a transformation is found such that an n^{th}-order problem can be replaced by a first-order problem, it can be shown that, for the transformed problem, perfect performance can be in principle achieved in presence of parameter inaccuracy. As a drawback, such performance is generally obtained at the price of higher control activity. Consider the following single-input/single-output (SISO) n^{th}-order dynamical system

$$\frac{d^n}{dt^n}x = f(\boldsymbol{x}) + b(\boldsymbol{x})u. \tag{12}$$

Here, x is the output state, u is the control variable, and $\boldsymbol{x} = [x, \dot{x}, \ddot{x}, \cdots, x^{(n-1)}]^T$ is the state vector. Both the nonlinear plant dynamics $f(\boldsymbol{x})$ and the control gain $b(\boldsymbol{x})$ are assumed to be not exactly known. Under the condition that both $f(\boldsymbol{x})$ and $b(\boldsymbol{x})$ have a known upper bound, the sliding control goal is to get the state $\boldsymbol{x}$ to track the desired state $\boldsymbol{x}_d = [x_d, \dot{x}_d, \ddot{x}_d, \cdots, x_d^{(n-1)}]^T$ in presence of model uncertainties. The time-varying sliding surface is introduced as a function of the tracking error $\tilde{\boldsymbol{x}} = \boldsymbol{x}$ - $\boldsymbol{x}_d = [\tilde{x}, \dot{\tilde{x}}, \ddot{\tilde{x}}, \cdots, \tilde{x}^{(n-1)}]^T$ by the following scalar equation

$$s(\boldsymbol{x}, t) = \left(\frac{d}{dt} + \lambda\right)^{n-1} \tilde{x}. \tag{13}$$

Here, λ is a strictly positive constant. For example, if $n = 2$ we obtain

$$s(\boldsymbol{x}, t) = \dot{\tilde{x}} + \lambda\tilde{x} = 0. \tag{14}$$

With the definitions in Eq. (13) and Eq. (14), the tracking problem is reduced to the problem of forcing the dynamical system in Eq. (12) to remain on the time-varying sliding surface. Clearly, tracking an n-dimensional vector $\boldsymbol{x}_d$ has been reduced to the problem of keeping the scalar sliding

surface to zero, i.e. the problem has been reduced to a first-order stabilization problem in s. The simplified first-order stabilization problem can be achieved by selecting a control law such that, outside the sliding surface $s(\boldsymbol{x}, t)$, the following condition is satisfied:

$$\frac{1}{2}\frac{d}{dt}s^2 \leq -\eta|s|. \tag{15}$$

Here, η is a strictly positive constant. Eq. (15), also called the "sliding condition", explicitly states that the distance from the sliding surface decreases exponentialy along all system trajectories. Generally, constructing a control law that satisfies the sliding condition is fairly straightforward. For example, using the Lyapunov direct method, one can select a candidate Lyapunov function as follows

$$V(s) = \frac{1}{2}s^T s. \tag{16}$$

Eq. (16) satisfies the following two conditions: $V(0) = 0$ and $V(s) > 0$ for $s > 0$. By taking the derivative of Eq. (16), it is easily concluded that the sliding condition (Eq. (15)) is satisfied. The control law is generally obtained by substituting the sliding control definition, Eq. (14), and the system dynamical equations, Eq. (12), into Eq. (15).

Multiple Sliding Surface Guidance Design

The circular restricted three-body problem (CRTBP) describes the dynamics of a massless body attracted by two point masses revolving around each other in a circular orbit. The overall approach to MSSG development for a CRTBP is to employ the notion that the motion of the guided spacecraft forced to exist in a 2-sliding mode. The following definition clarifies the concept:

Definition 1 *Consider a smooth dynamical system with a smooth output $s(\boldsymbol{x})$ (sliding function). Then, provided that $s, \dot{s}, \ddot{s}, \cdots, s^{r-1}$ are continuous and that $s = \dot{s} = \ddot{s} = \cdots = s^{r-1} = 0$, then the motion on the set $\{s, \dot{s}, \ddot{s}, \cdots, s^{r-1}\} = \{0, 0, 0, \cdots, 0\}$ is said to exist on a r-sliding mode.*

For a class of sliding surfaces that are of interest to guidance problems applied to the CRTPB, the dynamics of the system is such that the sliding surfaces are of order two. Let us define the first sliding vector surface in the following way

$$\boldsymbol{s}_1 = \boldsymbol{r} - \boldsymbol{r}_d. \tag{17}$$

Here, $\boldsymbol{r}_d$ is the position of the desired (target) point on the Halo orbit (insertion point). Taking the derivative of the $\boldsymbol{s}_1$, we obtain

$$\dot{\boldsymbol{s}}_1 = \dot{\boldsymbol{r}} - \dot{\boldsymbol{r}}_d = \boldsymbol{v} - \boldsymbol{v}_d, \tag{18}$$

where $\boldsymbol{v}_d$ is the desired landing velocity. The guidance problem can be formulated as a standard control problem: Find the acceleration command law such that, in a finite time t_F, $\boldsymbol{s}_1 \rightarrow \boldsymbol{0}$ and $\dot{\boldsymbol{s}}_1 \rightarrow \boldsymbol{0}$. It is easily verified that the sliding surface is of relative degree two:

$$\ddot{\boldsymbol{s}}_1 = \dot{\boldsymbol{v}} - \dot{\boldsymbol{v}}_d = 2\boldsymbol{w} \times \boldsymbol{v} + \boldsymbol{w} \times \boldsymbol{w} \times \boldsymbol{r} + \frac{\partial U^T}{\partial \boldsymbol{r}} + \boldsymbol{a}_c - \dot{\boldsymbol{v}}_d. \tag{19}$$

The guidance objective is achieved by setting $\dot{\boldsymbol{s}}_1$ as a virtual controller and using a backstepping approach. More specifically, $\dot{\boldsymbol{s}}_1$ is found such that the first sliding surface is driven to zero in a finite time. The virtual controller can be conveniently selected as

$$\dot{\boldsymbol{s}}_1 = -\frac{\boldsymbol{\Lambda}}{t_F - t}\boldsymbol{s}_1, \tag{20}$$

where $\boldsymbol{\Lambda} = diag\{\Lambda_1, \Lambda_2, \Lambda_3\}$ is a diagonal matrix of guidance gains. To drive the first sliding surface to zero, the virtual controller $\dot{\boldsymbol{s}}_1$ must be globally stable. The global stability of $\dot{\boldsymbol{s}}_1$ can be shown by choosing the following candidate Lyapunov function

$$V_1 = \frac{1}{2}\boldsymbol{s}_1^T\boldsymbol{s}_1. \tag{21}$$

Accordingly, V_1 has the following properties

$$\begin{aligned} V_1(\mathbf{0}) = 0 \qquad & if \quad \boldsymbol{s}_1 = 0 \\ V_1(\boldsymbol{s}_1 > 0 \qquad & \forall \boldsymbol{s}_1 \neq 0 \\ V_1(\boldsymbol{s}_1) \to \infty \qquad & if \quad \boldsymbol{s}_1 \to \infty. \end{aligned} \tag{22}$$

In addition, for stability, the time derivative of V_1 must be negative definite everywhere. Imposing positive guidance gains $\{\Lambda_1, \Lambda_2, \Lambda_3\} > 0$ and setting $\boldsymbol{s}_1 = \{s_{1i}, \quad i = 1, 2, 3\}$, one obtains

$$\dot{V}_1 = \boldsymbol{s}_1^T\dot{\boldsymbol{s}}_1 = -\frac{1}{t_F - t}\boldsymbol{s}_1^T\boldsymbol{\Lambda}\boldsymbol{s}_1 = -\frac{1}{t_F - t}(\Lambda_1 s_{11}^2 + \Lambda_2 s_{12}^2 + \Lambda_3 s_{13}^2) < 0. \tag{23}$$

However, it is generally desirable that the matrix gains are all greater than one to ensure that both sliding surface and its derivative approach zero in a finite time. Indeed, the time variation of the sliding surface vector s_1 can be explicitly derived as function of the guidance gains. Applying separation of variables to Eq. (20), one obtains

$$\frac{ds_{1i}}{s_{1i}} = -\frac{\Lambda_i dt}{t_F - t}, \tag{24}$$

where $i = 1, 2, 3$ are the components of the sliding surface vector. Eq. (24) can be integrated in closed form to obtain

$$\ln(s_{1i}) = \Lambda_i \ln(t_F - t) + C_i. \tag{25}$$

By imposing the initial conditions $\boldsymbol{s}_1(0) = \boldsymbol{s}_{10}$ and taking the exponential of both sides, the solution becomes

$$s_{1i}(t) = s_{1i}(t_F - t)^{\Lambda_i}, \tag{26}$$

or in vector form

$$\boldsymbol{s}_1(t) = \boldsymbol{s}_{10}(t_F - t)^{\boldsymbol{\Lambda}}. \tag{27}$$

The derivative of the sliding surface vector can be also explicitly derived as

$$\dot{s}_{1i}(t)\Lambda_i s_{1i}(t_F - t)^{\Lambda_i - 1}, \tag{28}$$

or in vector form

$$\dot{\boldsymbol{s}}_1(t) = \boldsymbol{\Lambda}\boldsymbol{s}_{10}(t_F - t)^{\boldsymbol{\Lambda}-\boldsymbol{I}}. \tag{29}$$

As it can be seen from Eq. (27), as long as $\Lambda_i > 0$ $(i = 1, 2, 3)$, the sliding surface vector will achieve zero in a finite time. However, if $\Lambda_i < 1$ $(i = 1, 2, 3)$, the derivative of the sliding surface vector goes to infinity for $t = t_F$. Therefore, if the matrix gains are selected such that $\Lambda_i > 1$ $(i = 1, 2, 3)$ both the sliding surface vector and its derivative go to zero as $t \to t_F$. At the time where the targeting maneuver for Halo orbit insertion is initiated, the spacecraft is generally characterized by position and velocity such that Eq. (20) is not satisfied. Importantly, to derive a meaningful guidance law, $\dot{\boldsymbol{s}}_1$ must be explictly linked to the acceleration command (or spacecraft thrust) that must be executed to drive both $\boldsymbol{s}_1$ and $\dot{\boldsymbol{s}}_1$ to zero. The subsequent idea is to define a second sliding surface vector such that an acceleration command can be found that drives s_1 from its initial state to a trajectory defined by the first-order non-linear equation Eq. (30). Moreover, it is required that the acceleration command maintains the system on the second surface until $\boldsymbol{s}_1$, $\dot{\boldsymbol{s}}_1 \to 0$ is achieved. The second sliding surface vector is defined in the following way

$$\boldsymbol{s}_2 = \dot{\boldsymbol{s}}_1 + \frac{\boldsymbol{\Lambda}}{t_F - t}\boldsymbol{s}_1. \tag{30}$$

Importantly, the new sliding surface vector is of relative degree 1 with respect to the acceleration command. It can be easily verified that the acceleration command appears explicitly within the expression of the first derivative of $\boldsymbol{s}_2$

$$\dot{\boldsymbol{s}}_2 = \ddot{\boldsymbol{s}}_1 + \frac{\boldsymbol{\Lambda}}{t_F - t}\dot{\boldsymbol{s}}_1 + \frac{\boldsymbol{\Lambda}}{(t_F - t)^2}\boldsymbol{s}_1. \tag{31}$$

Using Eq. (19) it is explicitly found that

$$\dot{\boldsymbol{s}}_2 = 2\boldsymbol{w} \times \boldsymbol{v} + \boldsymbol{w} \times \boldsymbol{w} \times \boldsymbol{r} + \frac{\partial U^T}{\partial \boldsymbol{r}} + \boldsymbol{a}_c(t) + \frac{\boldsymbol{\Lambda}}{t_F - t}\dot{\boldsymbol{s}}_1 + \frac{\boldsymbol{\Lambda}}{(t_F - t)^2}\boldsymbol{s}_1 - \dot{\boldsymbol{v}}_d. \tag{32}$$

The desired acceleration command $\boldsymbol{a}_c(t)$ (guidance law) is determined using a Lyapunov approach. Define a second Lyapunov candidate function as follows

$$V_2 = \frac{1}{2}\boldsymbol{s}_2^T\boldsymbol{s}_2. \tag{33}$$

The Lyapunov function V_2 satisfies conditions similar to the one defined for V_1 (see Eq.(22). Moreover, its time derivative can be explicitly computed as

$$\dot{V}_2 = \boldsymbol{s}_2^T\dot{\boldsymbol{s}}_2 = \boldsymbol{s}_2^T\{2\boldsymbol{w} \times \boldsymbol{v} + \boldsymbol{w} \times \boldsymbol{w} \times \boldsymbol{r} + \frac{\partial U^T}{\partial \boldsymbol{r}} + \boldsymbol{a}_c(t) + \boldsymbol{\Lambda}\frac{(t_F - t)\dot{\boldsymbol{s}}_1 + \boldsymbol{s}_1}{(t_F - t)^2} - \dot{\boldsymbol{v}}_d\}. \tag{34}$$

The acceleration command is selected as follows

$$\boldsymbol{a}_c(t) = -\{2\boldsymbol{w} \times \boldsymbol{v} + \boldsymbol{w} \times \boldsymbol{w} \times \boldsymbol{r} + \frac{\partial U^T}{\partial \boldsymbol{r}} + \boldsymbol{\Lambda}\frac{(t_F - t)\dot{\boldsymbol{s}}_1 + \boldsymbol{s}_1}{(t_F - t)^2} - \dot{\boldsymbol{v}}_d + \boldsymbol{\Phi} sgn(\boldsymbol{s}_2)\}. \tag{35}$$

Eq. (35) is the Multiple Sliding Guidance Law (MSSG) adapted to account for the dynamics typical of the CRTBP. The matrix coefficients $\boldsymbol{\Phi} = diag\{\Phi_1, \Phi_2, \Phi_3\}$ can be selected as

$$\Phi_i = \frac{s_{2i}(0)}{t_F^\star}. \tag{36}$$

Using Eq. (36), one can show that the second sliding surface vector is driven to zero in a finite time $t_F^\star < t_F$. In fact, by replacing the guidance law explicitly derived in Eq. (35) into Eq. (32), the dynamics of the second sliding surface vector becomes

$$\dot{\boldsymbol{s}}_2 = -\boldsymbol{\Phi} sgn(\boldsymbol{s}_2). \tag{37}$$

Noting that $\boldsymbol{s}_2$ does not change sign before reaching zero, Eq. (37) can be integrated between zero and t to yield

$$s_{2i}(t) = s_{2i}(0) - \frac{|s_{2i}(0)|}{t_F^\star}t. \tag{38}$$

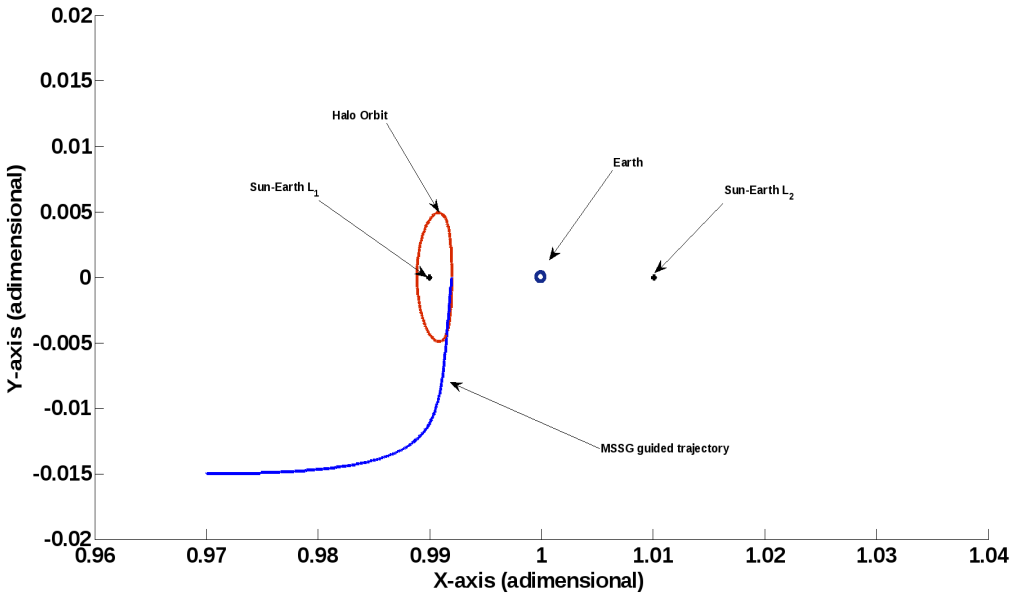

Figure 2. Halo orbit insertion at Sun-Earth L_1 Libration point.

Clearly, the second sliding surface vector goes to zero as $t \to t_F^\star$. Importantly, the derived MSSG law for Halo orbit insertion is globally stable. Inserting Eq. (35) into Eq. (34) and augmenting the

equations of motion to account for the perturbing acceleration, the Lyapunov function first derivative $\dot{V}_2$ becomes

$$\dot{V}_2 = \boldsymbol{s}_2^T \dot{\boldsymbol{s}}_2 = \boldsymbol{s}_2^T \{\boldsymbol{a}_p(t) - \boldsymbol{\Phi} sgn(\boldsymbol{s}_2)\} < 0. \tag{39}$$

The time derivative of the second Lyapunov function is always less than zero if an upper bound for the perturbing acceleration $\boldsymbol{a}_p^{MAX}$ is available. In such a case, the matrix coefficients $\boldsymbol{\Phi}$ can be selected such that $\Phi_i > |a_{pi}^{MAX}|$. The second Lyapunov function is therefore decrescent and by virtue of the Lyapunov stability theorem for non-autonomous systems $\boldsymbol{s}_2 \rightarrow 0$ as $t \rightarrow t_F^\star$. Consequently, $\boldsymbol{s}_1, \dot{\boldsymbol{s}}_1 \rightarrow 0$ as $t \rightarrow t_F$.

SIMULATION RESULTS

A novel non-linear guidance algorithm for spacecraft approaching a target vehicle in a halo orbit in the Sun-Earth system is presented. The guidance law formulation is implemented in the simulation plattform according to Eq. (35). MSSG has been implemented and simulated to verify the ability to target the insertion point of a suitable halo orbit around the L_1 point of the Sun-Earth system, as shown in Figure 2 (280,000 km radius is assumed). The guidance algorithm is required to drive the spacecraft in a halo orbit. The results show that the guidance scheme is able to successfully target a suitable state for proper orbital insertion. Furthermore, the MSSG algorithm can be used to target the L_1 point in the Sun-Earth system. The effect of the guidance matrix $\boldsymbol{\Lambda}$ on the guided trajectories is analysed. The simulations are initiated at $t = 0$ and conducted until approximately 70 days. Figure 3 shows the MSSG guided trajectory to the L_1 Libration point in the Sun-Earth system. The MSSG guidance gains are set to be $\boldsymbol{\Lambda} = diag\{2, 4.6\}$ for the simulations. The time evolution of the position is plotted in terms of components in Figure 4 (a) and Figure 4 (b) for the velocity. The acceleration variation components appears in Figure 5 for various guidance gains. The MSSG algorithm generates trajectories that can be subdivided in two phases. The acceleration command drives the second sliding surface to zero in the first phase of the flight ($0 < t < t_F^\star$). The second phase is initiated once the second surface is reached ($t = t_F^\star$). Thus, the first surface is driven to zero during this phase according to the nonlinear first-order dynamics given by Eq. (20). The magnitude of the acceleration command tends to increase for each of the three components with the guidance parameter, which regulates the rate at which the first surface is reached. Although the time of fligh is fixed, the rate of convergence depends on the parameter $\boldsymbol{\Lambda}$. The magnitude of the total acceleration command is shown in Figure 6. The time history of the sliding surface s_1 is depicted in Figure 7 (a) and Figure 7 (b) for s_2. The norm of the second sliding surface is driven to zero at $t = t_F^\star$ and maintained within a prescribed tolerance for the rest of the flight. The performances degradated for lower values of the guidance gains. The effect of the rate of convergence can be clearly seen in Figure 7 (a), in which the guidance parameter influences the shape of the sliding surface norm. The effects on the transfer time and Δ_v are plotted for 110 days in Figure 8. It should be noted that $t_F^\star$ has a strong influence in both shaping the trajectory and on the overall acceleration magnitude.

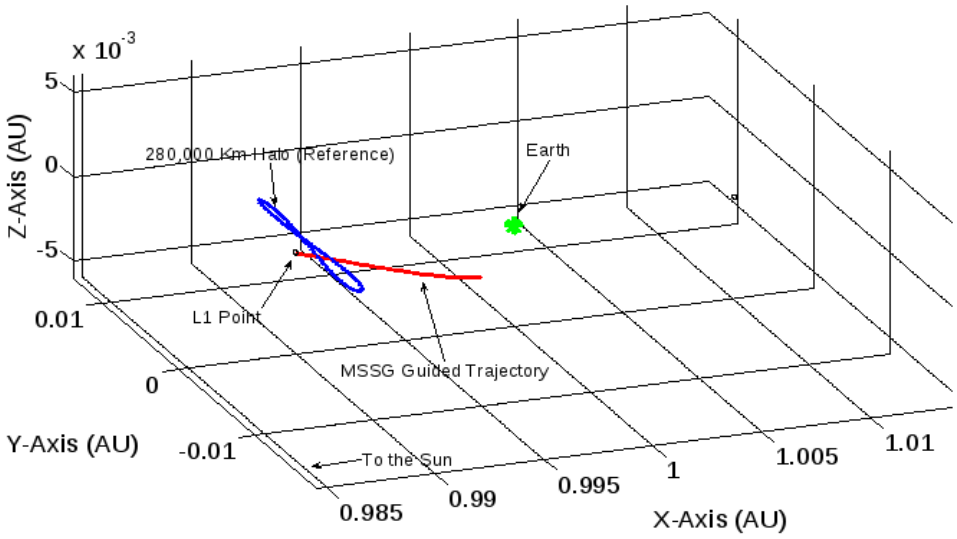

Figure 3. MSSG guided trajectory to the L_1 Libration point.

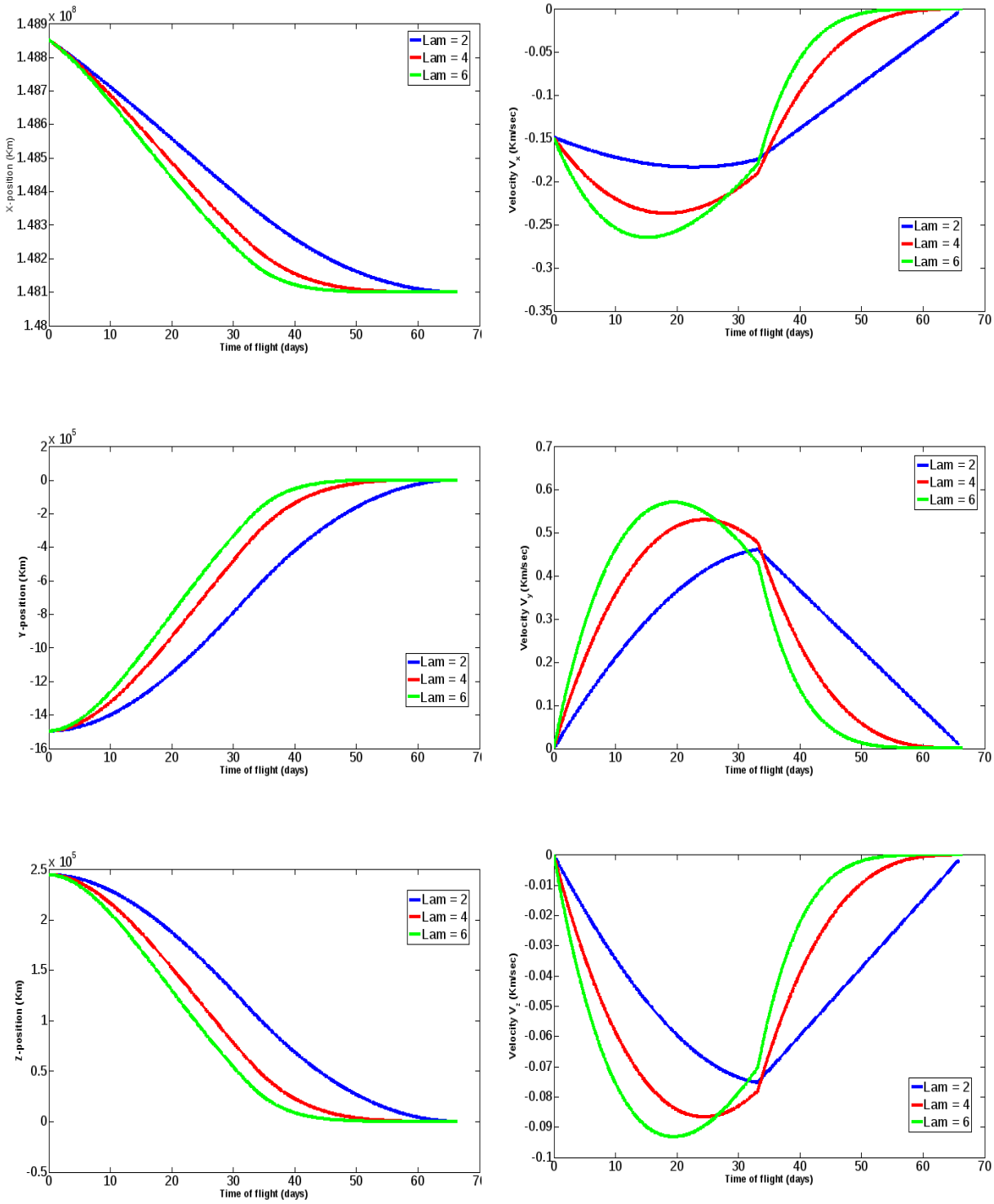

(a) (b)

Figure 4. (a) **Position variation components;** (b) **Velocity variation components.**

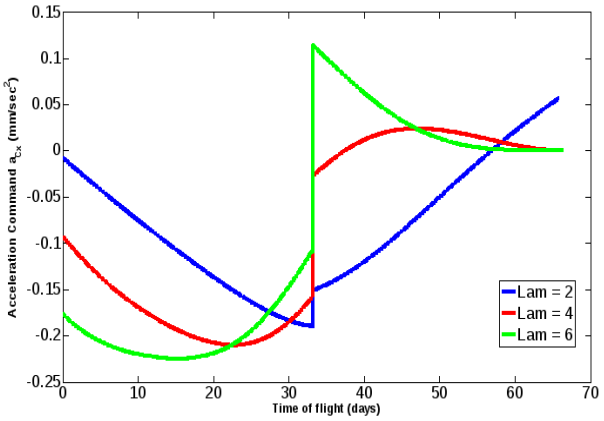

(a)

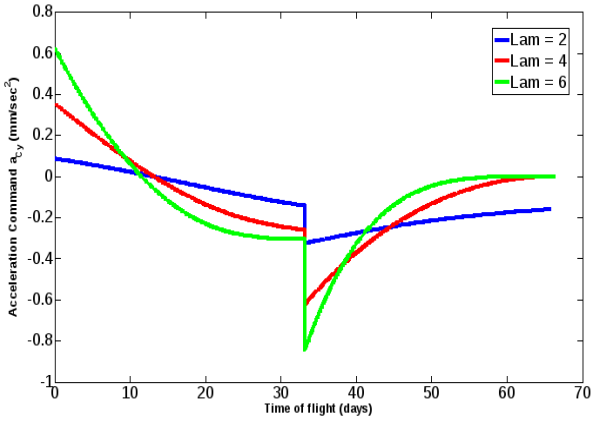

(b)

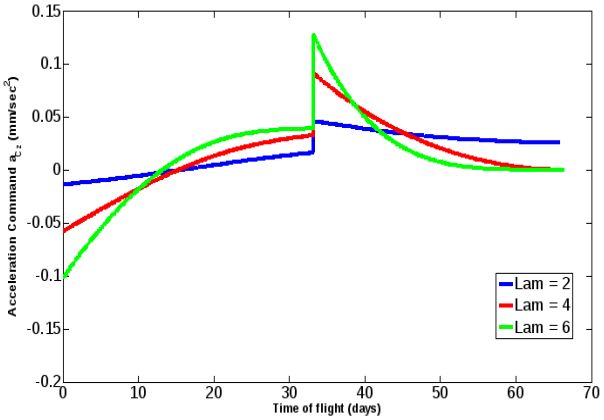

(c)

Figure 5. Acceleration variation components.

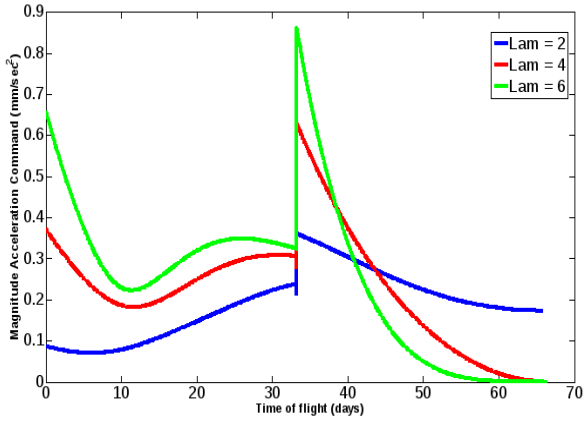

Figure 6. Magnitude of the total Acceleration Command.

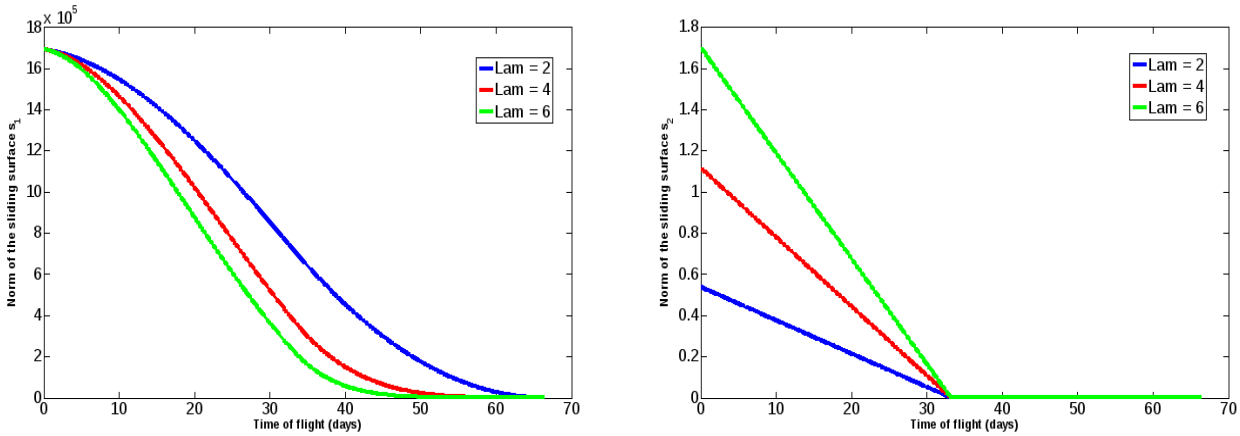

(a) (b)

Figure 7. (a) Sliding surface time response, s_1; (b) Sliding surface time response, s_2.

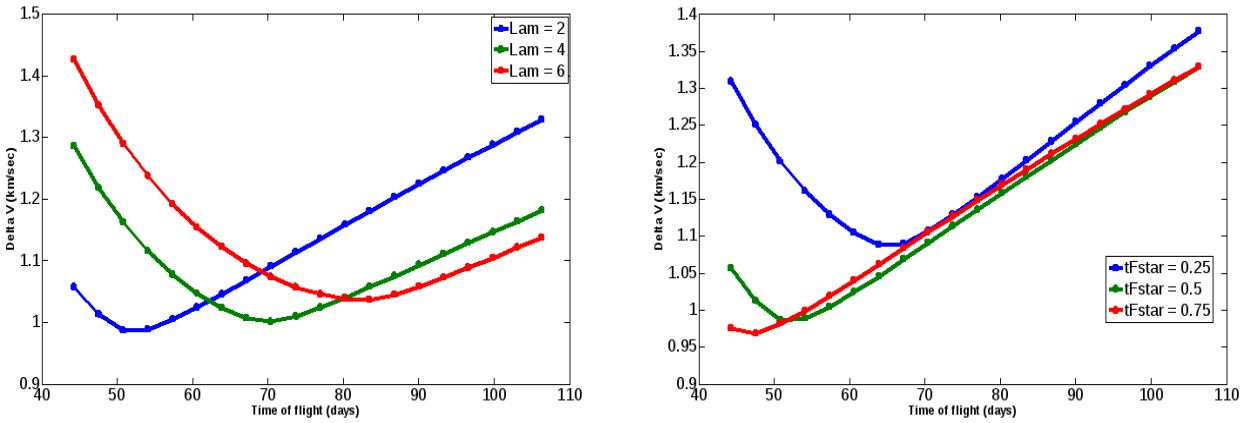

(a) (b)

Figure 8. (a) Δ_v sequence for $\mathbf{\Lambda} = diag\{2, 4, 6\}$; (b) Δ_v sequence for $t_F^\star = \{0.25, 0.5, 0.75\}$.

CONCLUSIONS

This paper studies the trajectory targeting and guidance problem in the Sun-Earth system. The proposed MSSG algorithm uses a HOSC theory and computes an acceleration command that target a specified state by considering only knowledge of the current and desired position and velocity. The discussion and practical application of the MSSG algorithm to target the insertion point of a suitable halo orbit in the vicinity of the Sun-Earth libration points has been presented. While not intended to be a complete investigation, a thorough halo orbit targeting should be made later. Moreover, a practical example of the algorithm to target the L_1 point in the Sun-Earth system has been demonstrated. The robustness of the algorithm against pertubations and unmodeled dynamics make it ideal for on-board targeting and guidance problem.

REFERENCES

[1] V. Szebehely, *Theory of Orbits: the Restricted Problem of Three-Bodies*. New York and London: Academic Press, 1967.

[2] A. E. Roy, *Orbital Motion*. Bristol and Philadelphia: Institute of Physics Publishing, 2005.

[3] R. Farquhar, "The Utilization of Halo Orbits in Advanced Lunar Operations," *Nasa technical report*, 1971.

[4] R. W. Farquhar and D. W. Dunham, "Use of Libration-Point Orbits for Space Observatories," *In Observatories in Earth Orbit and Beyond, Kluwer Academic Publishers*, 1990, pp. 391–395.

[5] D. L. Richardson, "A note on a Lagrangian Formulation for Motion about the Collinear Points," *Celestial Mechanics*, Vol. 22, 1980, pp. 231–236.

[6] K. Howell, "Three-Dimensional, Periodic, 'Halo' Orbits," *Celestial Mechanics*, Vol. 32, 1984, pp. 53–71.

[7] G. Gómez, A. Jorba, J. Masdemont, and C. Simó, *Dynamics and Mission Design near Libration Points*, Vol. III, IV. World Scientific Monograph Series in Mathematics, 2001.

[8] K. C. Howell and H. J. Pernicka, "A Station-Keeping Method for Libration Point Trajectories," *Journal of Guidance, Control, and Dynamics*, Vol. 16, No. 1, 1993, pp. 151–159.

[9] D. Folta and M. Beckman, "Libration Orbit Mission Design: Applications of Numerical and Dynamical Methods," *World Scientific*, 2003.

[10] J. Simo and C. R. McInnes, "Displaced Periodic Orbits with Low-Thrust Propulsion in the Earth-Moon System," *In* 19^{th} *AAS/AIAA Space Flight Mechanics Meeting*, Savannah, Georgia, February 8 - 12, 2009. AAS 09-153.

[11] J. Simo and C. R. McInnes, "Designing Displaced Lunar Orbits Using Low-Thrust Propulsion," *Journal of Guidance, Control and Dynamics*, Vol. 33, No. 1, January-February 2010.

[12] J. Simo and C. McInnes, "Feedback Stabilization of Displaced Periodic Orbits: Application to Binary Asteroid," *In* 22^{nd} *AAS/AIAA Space Flight Mechanics Meeting*, Charleston, South Carolina, January 29 - February 2, 2012. AAS 12-130.

[13] J.-J. E. Slotine and W. Li, *Applied Nonlinear Control*. Englewood Cliffs, New Jersey 07632: Prentice Hall, 1991.

[14] A. Levant, "Sliding Order and Sliding Accuracy in Sliding Mode Control," *International Journal of Control*, Vol. 58, No. 6, 1993.

[15] A. Levant, "Higher-Order Sliding Modes, Differentiation and Output-Feedback control," *International Journal of Control*, Vol. 76, No. 9/10, 2003.

[16] A. Levant, "Quasi-Continuous High-Order Sliding-Mode Controllers," *IEEE Transactions on Automatic Control*, Vol. 50, No. 11, 2005.

[17] A. Levant, "Construction Principles of 2-Sliding Mode Design," *Automatica*, Vol. 43, No. 4, 2007.

[18] Y. B. Shtessel and C. H. Tournes, "Integrated Higher-Order Sliding Mode Guidance and Autopilot for Dual-Control Missiles," *Journal of Guidance Control and Dynamics*, Vol. 32, No. 1, 2009.

[19] M. U. Salamci, S. P. Banks, M. K. O. Y. B. Shtessel, and C. H. Tournes, "Sliding Mode Control with Optimal Sliding Surfaces for Missile Autopilot Design," *Journal of Guidance Control and Dynamics*, Vol. 23, No. 4, 2000.

[20] C. H. Tournes, Y. B. Shtessel, and I. Shkolnikov, "Missile Controlled by Lift and Divert Thrusters Using Nonlinear Dynamic Sliding Manifolds," *Journal of Guidance Control and Dynamics*, Vol. 29, No. 3, 2006.

[21] A. Koren, M. Idan, and O. M. Golan, "Integrated Mode Guidance and Control for a Missile with On-Off Actuators," *Journal of Guidance Control and Dynamics*, Vol. 31, No. 1, 2008.

[22] R. Furfaro, S. Selnick, M. L. Cupples, and M. W. Cribb, "Non-Linear Sliding Guidance Algorithms for Precision Landing," *In* 21^{rd} *AAS/AIAA Space Flight Mechanics Meeting*, New Orleans, Louisiana, February 13-17, 2011. AAS 11-167.

[23] R. Furfaro and D. R. Wibben, "Asteroid Precision Landing via Multiple Sliding Surfaces Guidance," *In AAS/AIAA Astrodynamics Specialist Conference*, Girdwood, Alaska, July 31 - August 4, 2011. AAS 11-647.

[24] R. Furfaro, D. O. Cersosimo, and J. Bellerose, "Close Proximity Asteroid Operations using Sliding Control Modes," *In* 22^{nd} *AAS/AIAA Space Flight Mechanics Meeting*, Charleston, South Carolina, January 29 - February 2, 2012. AAS 12-132.

[25] D. R. Wibben, B. Gaudet, R. Furfaro, and J. Simo, "Multiple Sliding Surface Guidance for Planetary Landing: Tuning and Optimization Via Reinforcement Learning," *In* 23^{rd} *AAS/AIAA Space Flight Mechanics Meeting*, Kauai, Hawaii, February 10 - 14, 2013. AAS 13-328.